TAO, Vol. 10, No. 3, 543-568, September 1999

Structure and Motion of the Southwestern Taiwan Fold and Thrust Belt

Jih-Hao Hung[1], David V. Wiltschko[2], Huang-Chi Lin[1], John B. Hickman[2], Peng Fang[3] and Yehuda Bock[3]

(Manuscript received 20 August 1998, in final form 19 May 1999)

ABSTRACT

Surface and limited seismic data have been used to construct new cross sections across the southwestern Taiwan Fold and Thrust Belt. South of Chiayi, the best fit to the data is achieved if the detachment lies at a depth of 10 to 12 km, stepping up to about 6 km to the west. The Chukou fault and its extension to the south (Lunhou fault) are not the frontal structures in this area. Available data indicate the frontal structure may be composed of incipient reactivated normal faults in the north and triangle zones in the south. Published leveling data show that, whatever the structure, it is growing.

From north of Chiayi to the south the salient nature of the structures of the Foothills province include: 1) a considerable amount of pre-Miocene strata are involved in the deformation. The involvement of pre-Miocene decreases to the south, but the depth of the basal detachment does not change due to the thickening of the Miocene and younger section; 2) the involvement of pre-existing normal faults and consequent 'basement' highs affecting the trajectory of thrust ramps abruptly ends south of Chiayi, separated by buried transverse faults from, 3) the thick foreland synorogenic stratigraphic sequence rides passively above the duplex wedge. Current seismicity appears to have no correlation to the interpreted locations of faults, whether thrust, normal or strike-slip.

Preliminary GPS data from this portion of the fold and thrust belt indicates, as first shown by Yu and Chen (1994), that structures are generally moving westward with respect to the Chinese craton. However, our data show abrupt changes in horizontal velocity, not all of which are associated with mapped faults. There is a region of high horizontal velocity and strain rate to the east of the Chukou-Lunhou fault. On a finer scale, the velocities

[1]Institute of Geophysics, National Central University, Chungli, Taiwan, ROC

[2]Department of Geology and Geophysics and Center for Tectonophysics, Texas A&M University, College Station, TX, USA

[3]Institute of Geophysics and Planetary Physics, Scripps Institution of Oceanography, University of California, San Diego, CA, USA

can vary greatly over distances of as little as 10 km. Some thrust sheets appear to be rotating counterclockwise around a vertical axis whereas others appear to be moving uniformly westward. Horizontal velocities are uniformly low in the Coastal Plain although they increase from west to east into the region of folding and blind thrusting in the footwall of the Chukou-Lunhou fault. The eastward increasing of shortening velocity in the Foothills Belt implies that a common detachment exists at depth or thrusts in the east of the Chukou-Lunhou fault are also active or both.

(Key words: Active tectonics, Balanced cross sections, GPS method, Fold and thrust belt)

1. INTRODUCTION

The fold-and-thrust belt of southwestern Taiwan (Figure 1) is an active zone of compressional deformation. This area is characterized by short recurrence interval seismicity and millimeter to centimeter per year surface motion, particularly in the vicinity of the Chukou fault (CKF). The CKF and associated footwall structures mark the surface deformation front in southwestern Taiwan. Wu et al. (1979) attributed the large 1964 Chiayi earthquake (M_L= 6.5) to slip on the CKF. Many of the 17 destructive historical earthquakes (Cheng and Yeh, 1989) felt in the heavily populated Chianan Plain to the west may have been due to slip along the CKF as well. Both geological and topographical evidence indicate that the alluvial terraces located in the footwall of the CKF were tilted westward by the encroaching Chukou thrust to the east (Huang et al., 1994). More recent geodetic data have confirmed that southwestern Taiwan is converging relative to Penghu at a velocity ranging from 2.6 mm/y near the western coast to 4.0 cm/y to the east of the CKF in an approximate azimuth of 300° (Yu and Chen, 1998). Yu and Chen (1998) found very high strains in the vicinity of the CKF. The principal strains within regions which include the CKF apparently increase to the south.

Earthquake activity in southwestern Taiwan was presumably triggered by movement along the CKF. Nevertheless, the location and nature of the causative faults has remained enigmatic. For example, current seismicity located by the Central Weather Bureau Network (CWBN) appears to have no correlation to the interpreted locations of faults, whether thrust, normal or strike-slip (Hung, 1996; Wiltschko et al., 1997). Conversely, focal mechanism studies of the Tapu earthquake (M_L = 5.7, 1993, December 16) show that the mainshock and aftershocks occurred along an unknown blind backthrust (Shin, 1995). Near the epicentral areas, no major faults are recognized at the surface or in the shallow subsurface, and the annually surveyed GPS data show little or no coseismic surface motion (Yu and Chen, 1998). In this paper our purposes are to, 1) use reflection seismic, drilling and geophysical databases to construct balanced cross sections which interpret the subsurface structure and kinematics in the southwestern Taiwan Foothills Belt, and 2) combine the GPS data collected by us between 1996 and 1997 and by Yu and Chen (1998) between 1990 and 1997 to document surface displacement and strain rates of rapidly growing fold and thrust wedge of southwestern Taiwan and also to

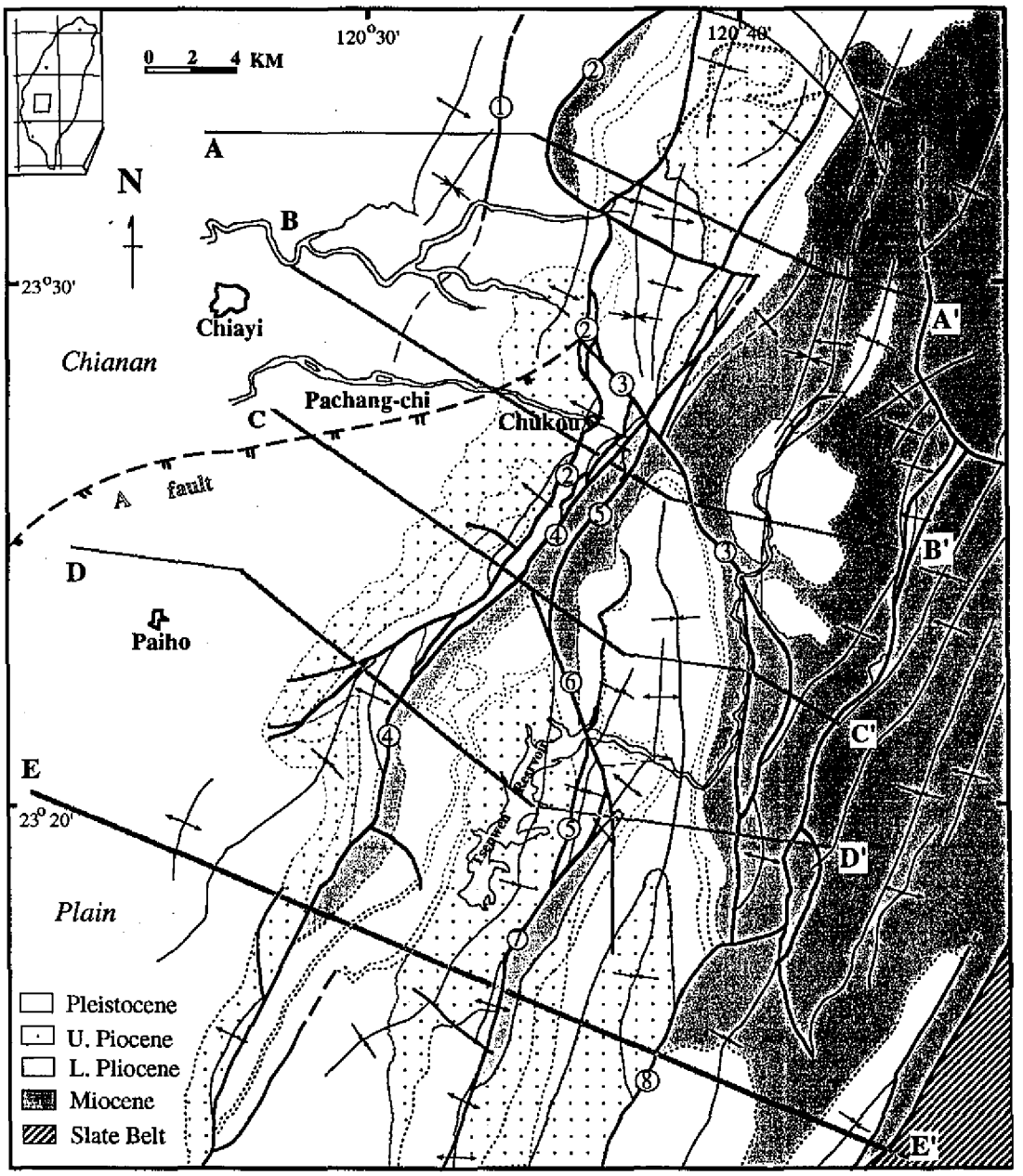

Fig. 1. Generalized geologic map of the southwestern portion of Taiwan showing the locations of the cross sections A-A' to E-E' (adapted from Chinese Petroleum Corporation, 1986, 1989). Major faults: 1. Chiuhsiungken, 2. Chukou, 3. Tatou, 4. Lunhou, 5. Matoushan, 6. Tingpinglin, 7. Chutouchi, 8. Pingchi.

document how individual structures are moving.

2. TECTONICS AND GEOLOGY OF SOUTHWESTERN TAIWAN

2.1 Stratigraphy

The surface geology of southwestern Taiwan foothills have been extensively studied by the Chinese Petroleum Corporation, Exploration Department (CPCED) and was mapped at a scale of 1:25,000 or 1:10,000. The Chinese Petroleum Corporation (CPC, 1986, 1989) has published two geological maps at a scale of 1:100,000. Stratigraphic relationships in southwestern Taiwan reflect a complex depositional and tectonic history, and it is not within our scope to discuss these relationships in detail. Interested readers should refer to Ho (1988) and Sun (1982) for a general review. The stratigraphy can be divided into tectono-stratigraphic facies that bracket the major tectonic events and provide the basic stratigraphic elements used in structural analysis in southwestern Taiwan.

At least two stages of rifting and a post-rifting orogeny occurred in the study area (Sun, 1982). The Paleocene-Eocene and Upper Oligocene to Pleistocene sedimentary sequences correspond to deposition associated with the first and subsequent stage of rifting that occurred at the Cretaceous-Paleocene and Eocene-Oligocene times, respectively. A major regional unconformity of the Early Oligocene age, encountered in both subsurface drilling and seismic profiles, separates the Late Oligocene or Miocene and above sequence from pre-Miocene rocks. The Paleogene strata were entirely or nearly removed by erosion, for example, in the Peikang basement high area, and the overlying Miocene rocks rest directly on the Paleocene or Cretaceous strata. The last stage of uplifting and rifting occurred in the Late Miocene and resulted in a disconformity in the Nanchuang Formation in many places to the west of the CKF based on subsurface wells and seismic profiles (Chow et al., 1986).

Extensive erosion coupled with systematic normal faulting (discussed below) results in an abrupt change of sedimentary facies and stratigraphic thickness across the grabens or sedimentary basins in the Chiayi-Tainan area (Yuan et al., 1984; Chow et al., 1986; Mao et al., 1994; Chang et al., 1996). At least three systems of lithostratigraphic units have established by the CPCED from field surveys along river profiles (CPC, 1986). The Alishan (column B, Table 1), which inherits the same stratigraphic units from northern Taiwan, is applied to the area north of the Pachang-chi. South of the Pachang-chi two other units, the Kuantzulin and the Tsenwen Reservoir (columns C and D, Table1, respectively) were used in the western and eastern regions of the Chukou-Lunhou fault. Biostratigraphic correlation among these lithostratigraphic units is made by means of calcareous nannofossils (column A, Table 1).

2.2 Structure

Surface structures in the study region were interpreted, previously, by Suppe (1976) as having a décollement-folding origin based on the fact that the same stratigraphic unit, namely, the Nanchuang Formation, appears immediately adjacent to major thrust faults in the hanging wall and extends along the fault trace for a considerable distance as well. Limited well infor-

Table 1. Nannobiostratigraphic correlation of stratigraphic systems in southwestern Taiwan (after Chi, 1980). Stratigraphy older than Nanchuang Formation is not exposed in the Kuangtzulin and Tsenwen Reservoir areas.

		A	B		C	D
Time		Martini's Zones (1971)	Alishan Area (Northern Taiwan)		Kuangtzuling (Yunshuichi)	Tsenwen Reservoir (Tsenwenchi)
Pleistocene		NN 21				
		NN 20	Tokoushan		Liushuang	Liushuang
		NN 19			Erhchungchi	Erhchungchi
					Kanhsialiao	Yuching
Pliocene	Late	NN 18	Cholan		Liuchungchi	Peiliao
		NN 17			Yunshuichi	Chutouchi
		NN 16				
	Early	NN 15	Chinshui			
		NN 14	Kueichulin	Tawo	Niaotsui	Maupu Ailiaochiao
		NN 13		Shiliufen	Chunglun	Yenshuikeng
		NN 12		Kuantaoshan		Tangyenshan
Miocene	Late	NN 11				
		NN 10	Nanchuang		Nanchuang	Changchihkeng Hunghuatzu Sanmin
	Middle	NN 9				
		NN 8				
		NN 7	Nankang	Kuanyinshan	Alishan System	
		NN 6				
	Early	NN 5		Talu		
		NN 4		Peiliao	Pa Chang Chi	
		NN 3	Shiti			
		NN 2	Taliao			
		NN 1	Mushan		Kuangtzuling System	Tsenwen Reservoir System
Oligocene	L.	NP 25	Wuchihshan			
		NP 24	Kankou			
	M.	NP 23	Szulin			
		NP 22				
	E.	NP 21				
Eocene	Late	NP 20	?		Chukou or Lunhou Fault	
		NP 19				
		NP 18			Unconformity	
		NP 17				

mation at the time allowed Suppe (1980, figures 7 to 10) to draw cross sections through structures in the study area. These sections show faults stepping from a décollement in the Miocene Nanchuang Formation to a higher décollement to form a convoluted imbricate stack of 1.5 to 2 kilometer thick packages of rock beneath anticlines. With the benefit of more recent seismic and well data (discussed below), it appears that 1) the Oligocene and other pre-Miocene strata are involved in the deformation and 2) the depth to the basal décollement horizon is several kilometers too high in Suppe's (1980) cross sections. Placing the basal fault at a deeper level thickens the stratigraphic package that must be imbricated to produce the surface structure and thus makes the subsurface structure much simpler.

Although thrusts and ramp anticlines are predominant surface structures in the foothills, normal faults may play a role in the compressive deformation during the orogenic event since the Pliocene. Normal faults trending east-west and north-south developed during several stages of tectonic rifting. For example the extensive east-west striking normal faulting under the Coastal Plain in the Peikang area were developed from the Late Cretaceous or the Early Paleocene through the Miocene (Chow et al., 1986; Mao et al., 1994). The east-west faults have been reactivated in largely strike-slip motion in historical earthquakes (Bonilla, 1975). Although north-south normal faults are less reported, they may exist in the foothills and connect with segments of east-west boundary normal faults (e.g., Hsu et al., 1980; Mao et al., 1994). Recent studies (e.g., Chang et al., 1996) show that north-south trending normal faults have been reactivated by thrusts. More detailed evidence indicating the existence and reactivation of normal faults in this area include:

(1) Abrupt changes of sedimentary facies and stratigraphic thickness that have occurred across the Chukou or Lunhou fault. For example, from surface mapping, the thickness of the Miocene Nanchuang (or Changchikeng) Formation changes from 250 m in the west to 750 m across the CKF (Chang et al., 1996; Figure 2, section A-A').

(2) An inverted structure which shows a reversal of stratigraphic separation appears on the upper part of the Hsiaomei fault (Figure 3). There is a change from normal separation on the pre-extensional and lower side of the syn-extensional units to reverse separation on the upper side of the syn-extensional units.

(3) The focal mechanisms of large earthquakes, for example, the Tapu earthquake (M_L= 5.7, Shin, 1995) and the Paiho earthquake (M_L= 6.5, Chang and Yeh, 1981), show that they occurred along steeply dipping reverse faults at depths greater than 10 km. These deep-seated steep reverse faults are uncommon in the fold and thrust belt and would be interpreted more properly as reverse-slip motion on pre-existing normal faults.

(4) High pore-pressure zones from the upper part of the Miocene Nanchuang Formation to the Pliocene Niaotsui Formation are encountered pervasively in wells drilled in southwestern Taiwan (Figure 4). Abnormally high fluid pressure may be required for normal faults to be reactivated as high-angle reverse faults (Sibson, 1985, 1995).

3. STRUCTURAL INTERPRETATION

The structural interpretation in the study area is primarily based on the construction of

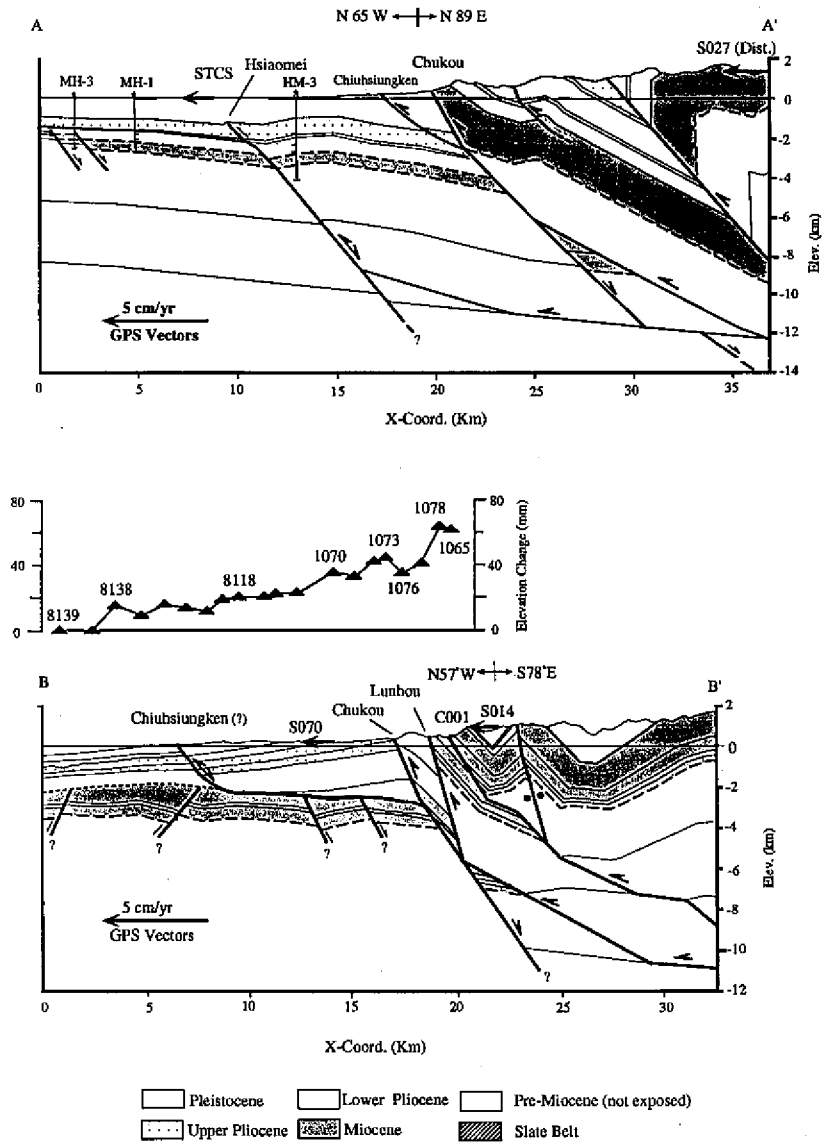

Fig. 2. Cross sections through Southwestern Foothills. Locations and drill depths of CPC wells used for interpretation and significant faults mentioned in text are labeled. Horizontal velocities of the GPS monuments are projected into the line of each cross section. The dense stations in section E-E' include data from Yu and Chen (1998). Repeated leveling during 1989/3 to 1992/7 along a transect through Chiayi is projected into section B-B' showing the relative elevation change of each station with respect to benchmark BM8139. The dashed line in each section indicates unconformity.

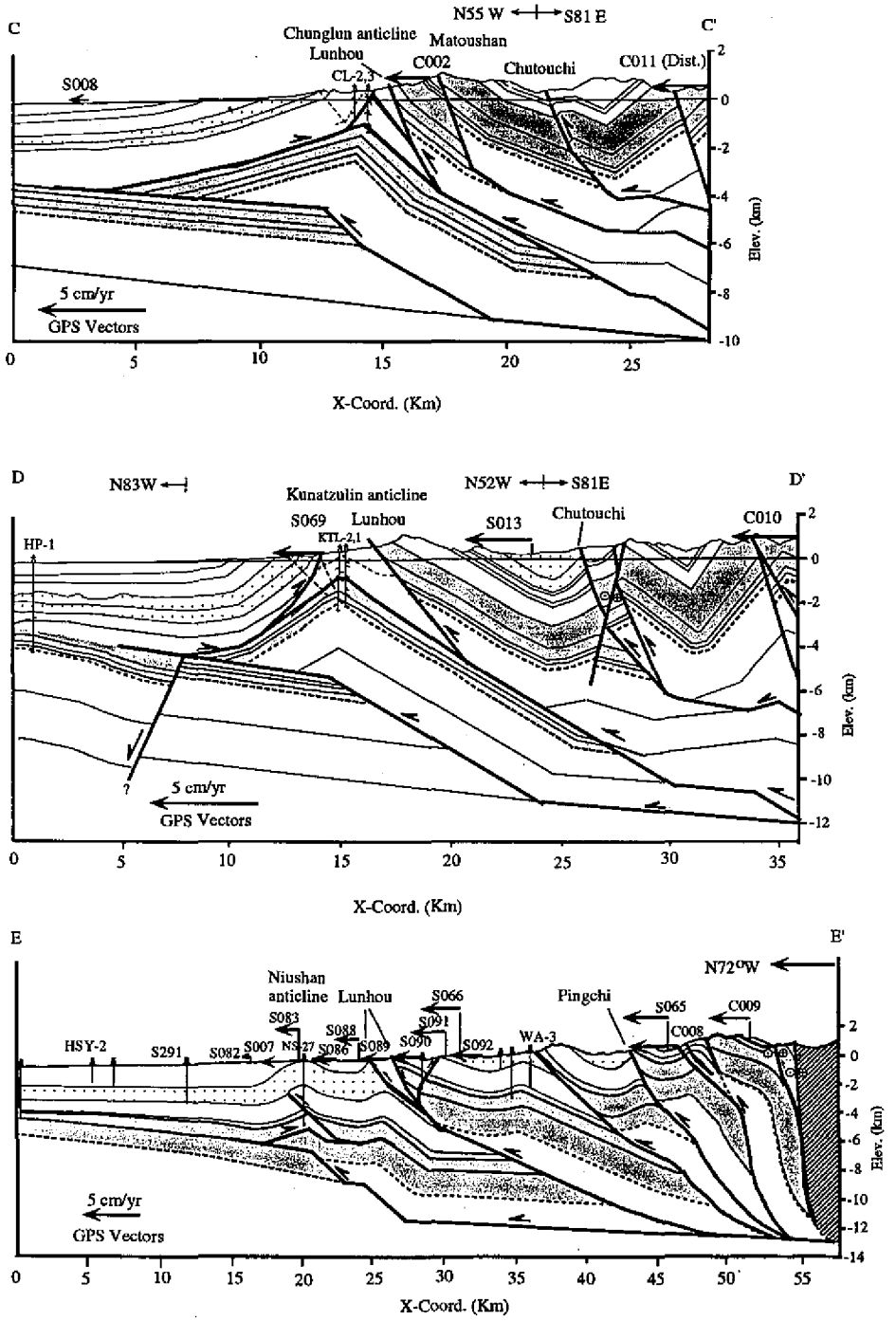

(*Fig. 2.* continued)

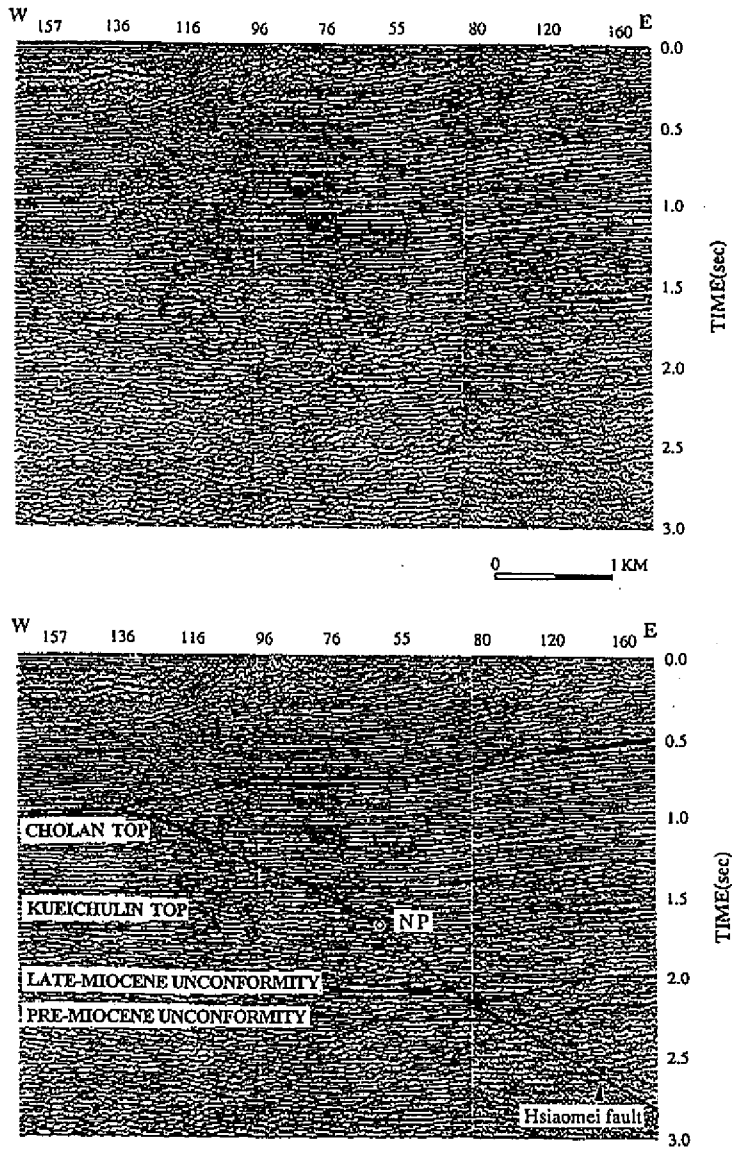

Fig. 3. Uninterpreted (A) and interpreted (B) seismic profiles showing an inverted structure along the upper part of Hsiaomei fault (located in the west of HM-3 in section A-A'). Note that the change of thickness across the fault mark the Late Miocene unconformity a boundary between pregrowth (strata below) and syngrowth sequences (strata above). With a small amount of reverse slip along the fault, the pregrowth unit is not entirely reversed, and the syngrowth sequence shows a normal separation on the lower side and reverse separation on the upper side with a null point (NP) of no separation in between.

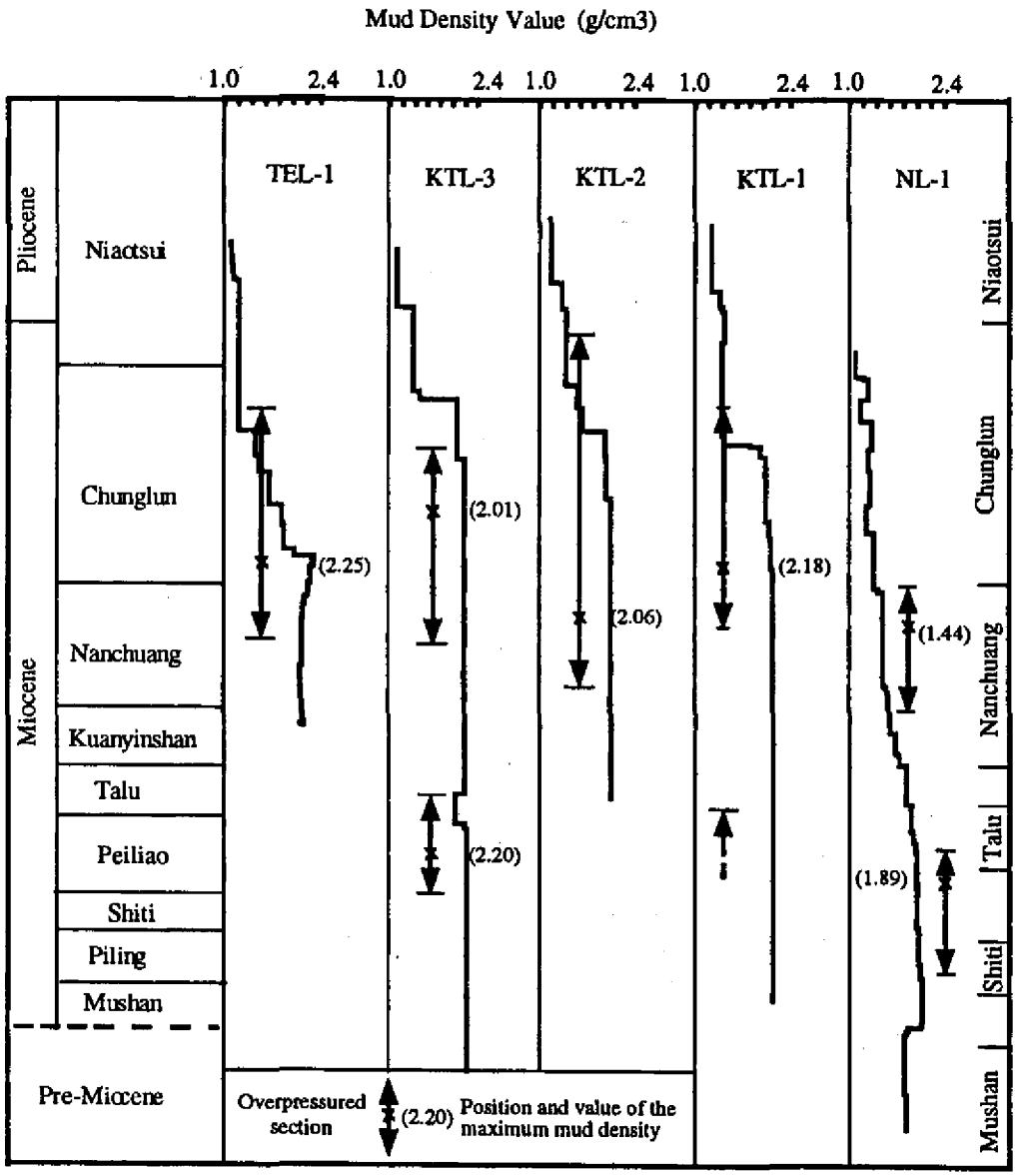

Fig. 4. Relationship between the mud density equivalent /depth value and stratigraphic horizon for representative wells in southern Taiwan (after Yuan et al., 1987). Note that the transition between hydrostatic and overpressured sections is nearly independent of well depth but is closely stratigraphically controlled, apparently due to low permeability of the overpressured sections. The stratigraphic horizon on the right side is for the NS-1 well.

kinematically restorable cross sections. Five cross sections (Figure 2) were chosen to make the most of the surface and subsurface geologic data and to pass through the GPS benchmarks (Figure 4). Published and unpublished geologic maps, seismic reflection profiles in the coastal plain, and subsurface wells from CPCED were assembled to construct the cross sections. Reactivation along normal faults was noted and incorporated in the cross sections. Other important constraints utilized for the cross sections include: a) P-wave velocity analyses from wide-angle seismic data across southern Taiwan (Lin et al., 1997; Shih et al., 1997) suggest that the boundary (Vp = 5 km/sec) between the basement and sedimentary cover is located at a depth from about 8 km in the Coastal Plain to 12 km in the foothills; b) backthrusts detached at the bottom of the Chunglun Formation appear in both the Chunglun and Kuantzulin anticlines (Hsu and Wei, 1983; Chang et al., 1996).

The Bouger gravity anomaly map displays local highs in frontal folds such as the Chunglun, Kuantzulin and Niushan anticlines (Yeh and Yen, 1992). The gravity highs were attributed to paleobasement highs (horst) developed in the Oligocene when extensive rifting occurred in southwestern Taiwan (Chang et al., 1996). Alternatively, duplex structures in which pre-Miocene strata are duplicated can also yield local gravity highs. Gravity modeling may help to provide some clarification. To conform with all available data and consistent among cross sections, we have chosen a décollement-folding origin to explain the surface structures. The basal detachment horizon is accordingly placed near the sedimentary cover/basement boundary. Based on the distinct frontal structures, cross sections A-A' to E-E' are divided into two groups with a detailed discussion below.

3.1 Sections A-A' and B-B'

Salient features in both A-A' and B-B' sections (Figure 2) include: a) normal faults have resulted in abrupt thickening of syngrowth strata in the hanging wall, and b) blind faults and overlying folds appear in the Coastal Plain. The CKF, although the most western exposed, is not the deformation front. Normal faults developed in the Coastal Plain prior to the Late Miocene unconformity are not affected by the compressive deformation encroaching from the east. By contrast, normal faults developed after the Miocene such as the Chukou, Hsiaomei faults in section A-A' and the Chiuhsiungken fault in section B-B' are reactivated. The high-angle CKF is interpreted to be caused by a reverse slip on a normal fault which developed from the Miocene until the Pleistocene Cholan Formation (compare corresponding stratigraphic thickness across the CKF), with the normal separation estimated over 3000 m from the accumulated stratigraphic thickness. The reverse slip along the CKF in section A-A' is about 11 km.

Hsiaomei anticline is a broad, relatively symmetric fold with low structural relief. It is a growing structure associated with a small amount of reverse slip along upper portions of the original normal fault, the Hsiaomei fault (Figures 2 and 3). Along the fault trace the change from reverse separation in strata above the Kueichulin top to normal separation in strata below the Late Miocene unconformity will pass through a null point with no separation in between (Mitra, 1993). Deep drilling in the HM-3 well and seismic profiles indicate that a significant amount of pre-Miocene strata is involved in the deformation. Both Hsiaomei and Chukou

faults are rooted in Cretaceous or older rocks, and may be detached from the sedimentary cover/basement horizon. During reverse slip, new ramps may be nucleated as thrust faults step up from the basal detachment and slip along the upper portions of older normal faults. The abandonment of lower steep normal-fault ramps and nucleation of new imbricates in the hanging wall in response to stress concentration to achieve a smoother thrust trajectory has been demonstrated separately in rock (Serra, 1977), sand and clay models (Hung, 1995).

The surface trace of the CKF marks the change in fault displacement. Analyses of fault slip and stratigraphic separation diagrams along fault traces show that displacement transfer may occur between the Chukou and Lunhou faults (Lin, 1996). The southward progressive decrease of stratigraphic separation and reverse slip along the CKF is gained by the Lunhou fault. In section A-A', it is known that the Chukou thrust cuts the 800,000 year old Tokoushan Conglomerates. Three tiers of alluvial terraces to the west of the CKF are interpreted to be related to its motion (Huang et al., 1994). The youngest terrace was deposited about 38,000 years ago based on C-14 dating. Faults to the east of the CKF are not dated yet; nevertheless current earthquake seismicity is more active to the east of the CKF. The displacement transfer between the Chukou and Lunhou faults indicates that if the Chukou is active, the Lunhou may also be active. Repeated leveling data on section B-B' show that the area including the west of the CKF is currently growing. The average tilting is at a rate of about 1 μradian/yr between BM 1078 and BM 8139, the amount of uplift increasing to the east (Yu, 1993).

3.2 Sections C-C' to E-E'

Among a systematic of east-west trending and south-dipping normal faults, which developed from the Middle Miocene to the Pleistocene in the southern rim of the Peikang basement high, the "A" fault (CPC, 1986; Figure 1) has the largest displacement and is recognized as a marginal fault (Chow et al., 1986, 1987). The "A" fault, primarily defined in the Coastal Plain, may have extended eastward into the foothill area and connects with the Chukou-Lunhou fault (Mao et al.,1994), but is less obvious due to lack of seismic data. Both the along strike termination of frontal fold and faults in sections A-A' and B-B' and the abrupt change of sedimentary facies across the "A" fault (Chang, 1963, 1964; Yeh et al., 1997) indicate that this blind transverse normal fault may play an important role as a boundary separating contrasting structural styles and stratigraphic sequences. The thickening of the Miocene and younger section to the south results in the change of deformation style from B-B' section to C-C' section in that the involvement of pre-existing normal faults and consequent 'basement' highs affecting the trajectory of thrust ramps (e.g., Wiltschko and Eastman, 1983) abruptly ends.

Sections C-C' and D-D' show uplifted tight folds, the Chunglun and Kuantzulin anticlines respectively, immediate to the west of the Lunhou fault. Both folds are formed by a deep simple step from the pre-Miocene strata to the upper detachment Chunglun Formation. Gravity data (Hu, 1985) and drilling suggest that the structural relief is higher on the Kuantzulin anticline than the Chunglun anticline. A minor thrust fault which cuts across the Chunglun Formation has been encountered in the CL-3, KTL-1, and KTL-2 wells (see Suppe, 1980; Hsu and Wei, 1983; unpublished CPC well-drilling reports). Repetition of strata is not clearly defined in the well log, and thus the thrust appears to be bedding-parallel, branching from the

Lunhou fault. No major strata repetitions or thrust faults are recognized at the surface to the west of the Chukou or Lunhou faults. Therefore the fault responsible for the Chunglun and Kuantzulin anticlines does not reach the surface but extends underneath the fold. The displacement on the fault may either extend out into the Coastal Plain to the west or transfer back to the east on an upper bed-parallel back thrust. The latter solution is indicated by, 1) the appearance of backthrusts along the Chunglun Formation in the outcrop and 2) no other frontal structures accommodating the slip to the west.

Frontal folds such as the Chunglun and Kuantzulin anticlines in southwestern Taiwan may be similar in geometry to a passive-roof duplex (Morley, 1986) or Type II triangle zone (Couzens and Wiltschko, 1996) which requires a thrust sheet injecting itself into the stratigraphic section at a middle or upper level. As shown by Couzens and Wiltschko (1996), the mechanical contrast between the cover sequence and the duplex units is a key factor in the formation of the Type II triangle zone, and the roof detachment appears to be located within the zone of the transition from mixed illite and smectite to illite-dominant clay in the shale. Although the mechanics of rocks in southwestern Taiwan have not been systematically tested, the lithology of Miocene and younger synorogenic sequence consisting of mainly marine mudstone and shale is presumably weaker than the brittle, indurated sandstone in the lower- and pre-Miocene strata. Increase of illite index (ratio between illite and mixed-layer clays such as smectite content) with depth are found within the abnormally high pore-pressure zones between upper Nanchuang and Niaotsui Formations (Yuan et al., 1987). Both characteristics may explain the formation of triangle zones as frontal structures and the Chunglun Formation as the upper detachment.

A triangle-zone geometry was applied to the buried deep part of the Niushan anticline in section E-E' although both in the lower stratigraphy and at a greater depth. Another deeper but less common high pore-pressure zone between the Talu and Shiti Formations (Figure 4) found in KTL-1 and NL-1 (south of the line of the section D-D') wells as well as thickening of the Neogene strata may explain why the blind structure developed in the deeper stratigraphy. This incipient triangle zone may indicate how the blind structures in sections C-C' and D-D' have begun. A complication in the Niushan anticline is that a fault-propagation fold may have formed above the triangle zone. This interpretation is favored by, 1) the asymmetry of the anticline with steep western limb as indicated by surface survey and gravity data; 2) the fact that an east-dipping thrust fault was encountered in well NS-27 at 3350 m, and that this fault does not crop out the surface. The involvement of pre-Miocene strata decreases in section E-E' but the depth of the basal detachment does not change due to the thickening of the Miocene and younger sections to the south (Yeh et al., 1997).

Displacement along the CKF is further reduced in section C-C' from B-B', and the CKF may merge with the Lunhou fault at a shallow depth. The backthrust in the Chunglun anticline cuts across the CKF and places older strata to the west overlying the younger strata to the east (Hsu and Wei, 1983; Huang et al., 1994). This cross-cutting relationship suggests that the backthrust is a younger fault and that CKF dies out underlying the Chunglun or Kuantzulin anticline. Consequently, displacement transfer may occur between CKF and faults to the east including the Lunhou fault. The partition of displacement among faults in this region suggests that it is out-of-sequence. The complicated fold geometry and high cut-off angle in the hang-

ing wall of the Chukou-Lunhou thrust in sections B-B' to E-E' is best explained by the Chutouchi fault (see section D-D') lopping off a pre-existing fold. Left-lateral strike-slip motion may develop associated with the break-back thrusting, particularly on the eastern most faults near the vicinity of the Fold and Thrust/Slate Belt boundary (Ho, 1988).

4. SURFACE MOTIONS FROM GPS

The Global Positioning System (GPS) is a useful tool for the study of crustal deformation in the regions of active tectonics. It is now possible to routinely quantify surface motion with millimeter precision at a variety of baseline scales (e.g., Bevis et al., 1993; Reilinger et al., 1997; Smith et al., 1994). The horizontal shortening rates in Taiwan are on the order of cm/yr across the island (Yu and Chen, 1994) and therefore statistically significant results can be expected after only two measurement epochs separated by one year or less. Because major structures appear to be active to a less or greater extent, it is feasible to examine the development of the actively growing fold and thrust belt in southwestern Taiwan.

4.1 Data Acquisition and Processing

We have installed ten new monuments (Figure 5) and collected data during two campaigns (1996 and 1997) at these monuments as well as other sites within the Southern Taiwan GPS network (Yu and Chen 1994). To better resolve the vertical component of motion, we occupied each site for at least 8 hours per session for short baselines (< 15km) and greater than 24 hours for long baselines. In addition, each site was occupied at least three times during a campaign with a geodetic dual-frequency GPS receiver (Trimble 4000SSE/SSI Geodetic Surveyor, one SST in 1996) tracking as many satellites as were in view. Established tracking stations (S01R, S23R, TAIW) were incorporated to maximize the geographic coverage of each field effort. Quasi-permanent stations were deployed in each campaign to provide another set of daily solutions to be averaged with the on-line tracking stations and thus reduce errors. The baselines by this method is kept under 50 km, and 25 km in most instances.

Data processing was carried out with GAMIT (King and Bock, 1995) software using a weighted least square method in full network mode (not baseline mode). The precise empherides were provided by the Scripps Institution of Oceanography of the University of California, San Diego, U.S.A. (SIO) and the International GPS Service for Geodynamics (IGS). A group of the IGS global tracking stations were included in the daily solutions to tie Taiwan regional sites to ITRF94 (Boucher et al., 1996) global reference frame. Tropospheric zenith delay parameters were estimated once per hour simultaneously using Niell's mapping function (Niell, 1996) with elevation cutoff set at 7 degree. In addition, IGS antenna phase center corrections and the solid earth tide correction terms were applied. After single daily sessions were processed, they were combined into one multi-session solution using a Kalman filter approach to generate site position series and velocity vectors with GLOBK (Herring, 1998) software. Analyzing the GPS data indicates that the vertical component is the most poorly determined, usually 3-4 times worse than the horizontal components in this area (Wiltschko et al., 1997; Yu

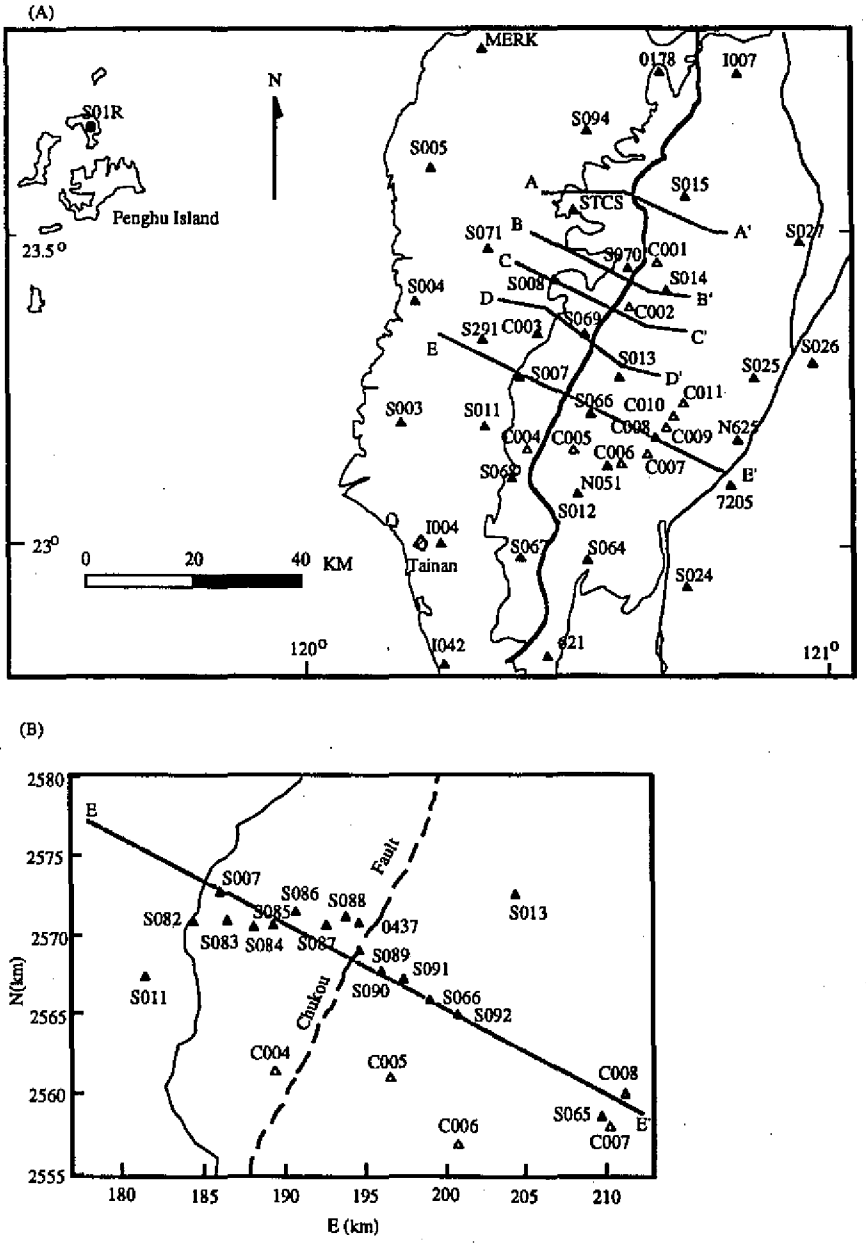

Fig. 5. (a) GPS monuments in southwestern Taiwan. Open triangles are new GPS monuments (site name starting with "C") and preexisting monuments of the Southern Taiwan GPS Network ("S") are solid triangles. S01R in the Penghu Island is continuous monitoring fixed station. The thick line is Chukou-Lunhou fault. (b) Locations of the dense monuments deployed along the route 174. A portion of the line of the section E-E' is shown.

and Chen, 1998). Since our two-year data are very preliminary, only horizontal components are discussed.

4.2 Horizontal Velocity

All station velocities are estimated relative to Paisha, Penghu (S01R), which is considered to be part of the stable Eurasian Continent. Station velocities with east and north components are listed in Table 2 and shown in Figure 6. Sites with large errors are not plotted. The pattern of horizontal velocities follows that described by Yu and Chen (1994): 1) a general decrease in velocity going from eastern to western sites, 2) a fan-shaped displacement pattern is observed in the frontal portion of the fold-and-thrust belt.

However, there are several additional observations that may be made from this dense network. First, there is considerable variation in horizontal velocity across the region. While rocks are generally moving in an arc from due west on the east side to more southwesterly on the west coast, there is an increased velocity in the vicinity of the Chukou-Lunhou fault. For example, there is a large velocity discontinuity (19.4 mm/yr) from sites S007 to S066 (Table 2). A comparable amount of increase in velocity was also observed by Yu and Chen (1994) and Yu and Chen (1998). Within the Foothills Belt, there exists a trend of increasing in velocity from north (S014, 17.6 mm/yr) to south (S064, 42.7 mm/yr) and from northwest (S091, 18.4 mm/yr) to southeast (7205, 47.6 mm/yr) across the Laonungchi fault. Also within this area, there appears to be large gradients in both velocity orientation and magnitude, for example, between sites C007 and C008. This implies that thrust sheets appear to be rotating around a vertical axis rather than moving uniformly to the west. The difference may be due to the fact that we have constructed smaller strain nets.

The rate of deformation estimated from geodetic data is consistent with geologic observations of deformation over a longer time period. For comparison, we have projected onto each section the horizontal velocity components parallel to the section line for GPS stations within 5 km of each section line (Figure 5). The total reverse displacement on the CKF measured in section A-A' is about 11 km, and the motion should be no earlier than 0.8 Ma (Huang et al., 1994). Therefore, the average slip rate is 14 mm/yr. Other independent study of the cross section in this area (Mouthereau et al., 1996) confirms a similar amount of average displacement velocity (11 mm/yr). This geologically determined finite displacement velocity is on the same order with the nearby GPS determined instantaneous shortening rate, 14.7 $\pm$ 1.9 mm/yr at station S014. Within the error of both the geologic and GPS estimates, there is at least qualitative confirmation that the Chukou thrust sheet is actively moving even though the surface trace is not. Although the agreement between the two independent measurements is rather good, caution is required to extrapolate two years of satellite observations to longer timescales of average deformation.

Our knowledge about the interplay between faulting and folding in the fold-thrust belt structures is limited. Consequently, the correlation of surface motions with individual structures shown in the cross sections is difficult. However, from the pattern of the horizontal shortening rate, tentative conclusions can be made. First, the relatively low velocities for sites in the Coastal Plain indicate that west extension of blind thrusts into the Coastal Plain is lim-

Table 2. Horizontal velocity of GPS stations relative to Paisha (S01R).

Station	V (mm/yr)	VE (mm/yr)	VN (mm/yr)	Azimuth (degree)
		Coastal Plain		
STCS	17.9±2.6	-17.4±2.0	-4.4±1.7	256
S070	19.5±2.2	-19.4±1.7	-2.4±1.4	263
S008	13.0±2.3	-11.0±1.7	7.0±1.6	302
S004	9.6±2.8	-9.2±2.0	-2.8±1.9	253
S291	5.7±3.6	-2.1±2.8	-5.3±2.3	202
S007	14.3±1.9	-14.0±1.5	-3.1±1.2	258
S011	16.9±1.4	-16.9±1.1	-0.9±0.8	267
S003	5.2±3.7	0.3±2.7	5.2±2.5	183
N601	9.6±1.7	-8.3±1.4	-4.8±1.0	240
S068	10.0±2.5	-9.8±1.9	-1.8±1.6	260
I004	15.7±3.1	-15.6±2.4	-1.9±2.0	263
		Foothills Belt		
S014	17.6±2.0	-17.6±1.5	0.7±1.3	272
C002	25.0±3.2	-23.2±2.4	9.2±2.1	292
S069	22.6±2.8	-22.4±2.0	3±1.9	278
C011	28.7±2.5	-28.4±1.9	-4.4±1.6	261
S013	33.4±1.5	-33.3±1.1	2.1±1.0	274
C009	39.4±2.2	-39.4±1.7	-0.6±1.4	269
C010	31.9±2.3	-31.9±1.7	-0.9±1.5	268
S088	25.5±3.9	-25.5±2.9	1.4±2.6	273
S089	10.1±2.7	-9.5±2.0	-3.3±1.8	251
S091	18.4±3.4	-16.9±1.1	-7.2±2.3	247
S092	32.9±2.9	-32.8±2.2	2.6±1.9	275
C008	39.8±2.1	-37.7±1.6	12.7±1.4	289
S066	33.7±2.1	-33.7±1.6	0.6±1.3	271
C005	13.6±2.0	-13.0±1.5	-3.9±1.3	253
C007	54.9±2.3	-49.3±1.7	-24.1±1.5	244
N051	45.4±1.6	-45.0±1.3	-5.8±0.9	263
C006	36.9±1.4	-35.7±1.1	-9.3±0.8	255
S012	30.2±1.8	-29.7±1.4	-5.4±1.2	260
S067	32.3±2.9	-26.5±2.0	-18.4±1.8	235
S064	42.7±3.5	-42.2±2.6	-6.6±2.4	261
621	52.9±3.7	-51.6±2.8	-11.7±2.4	257
S23R	47.2±1.0	-46.5±0.9	-8.3±0.5	260
		Central Range		
S027	21.9±2.8	-21.8±2.1	-1.6±1.9	266
S025	35.9±1.2	-35.9±1.0	-1.7±0.7	267
S026	21.5±1.2	-21.0±1.0	4.6±0.7	282
7205	47.6±2.5	-47.5±1.0	-2.2±1.6	267
N625	42.6±2.1	-40.2±1.7	-14±1.3	251

VE and VN are east and north components with positive values representing eastward and northward motions, respectively. V is the resultant velocity. The azimuth of the velocity vector is measured clockwise from the north.

ited. This observation is consistent with our interpretation of subsurface structures, in which thrusts stop at frontal structures and do not extend far west beneath the Coastal Plain. Second, the eastward progressive increase of velocity for the stations located in the hanging wall of the Chukou thrust in section E-E' (from 5.2 mm/yr at site S003 to 47.6 mm/yr at site 7205) implies

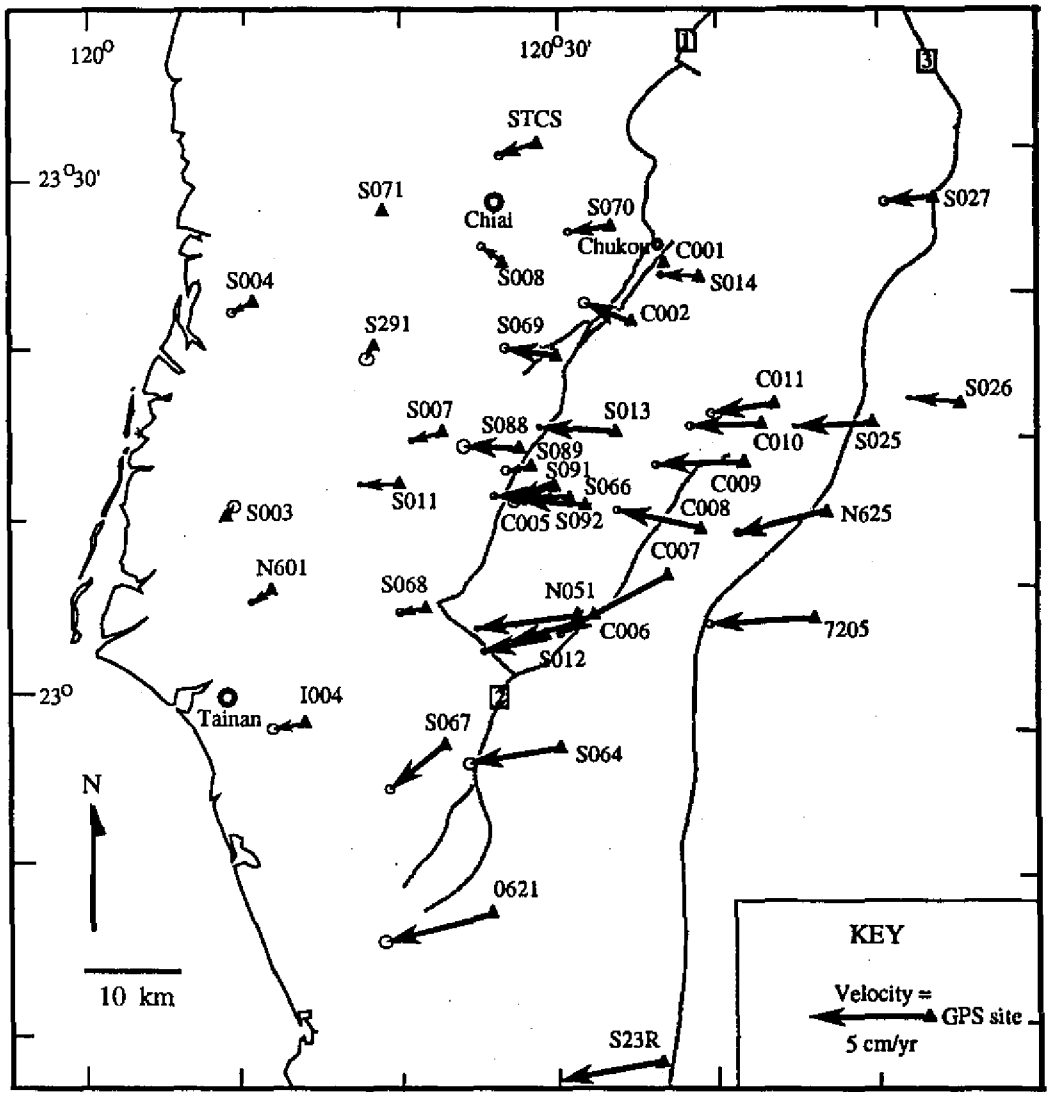

Fig. 6. Horizontal GPS station velocity relative to Paisha (S01R) in southwestern Taiwan. The 95% confidence ellipse is shown at the tip of each velocity vector. Gray lines are major thrust faults, 1: Chukou-Lunhou, 2: Pingchi, 3: Laonungchi.

that the crustal shortening is accumulating rapidly in the Foothills Belt and that the motion is not solely along the CKF (e.g., Yu and Chen, 1998). That is, synchronous movements on the faults located east of the CKF contribute to the eastward increase of the surface velocity. This observation is in concert with both the significant out-of-sequence thrusting required to restore our cross-sections and the earthquake activity in this region.

4.3 Strain Rate

To understand the spatial variation of strain in the study area, the GPS network is divided by triangular subnets, and strain rate tensors within each triangle are calculated from the horizontal velocity field assuming that strain within each triangle is homogeneous. The relationship between horizontal velocity vectors and surface strain is given in terms of strain rate tensor $\dot{E}$ through decomposition:

$$\dot{E} = \sum_{i=1}^{2} \dot{\varepsilon}_i \hat{e}_i \hat{e}_i^T$$

where $\dot{\varepsilon}_i$ are the eigenvalues and $\hat{e}_i$ are the eigenvectors:

$$\hat{e}_1 = \begin{bmatrix} \cos\theta \\ -\sin\theta \end{bmatrix} \qquad \hat{e}_2 = \begin{bmatrix} \sin\theta \\ \cos\theta \end{bmatrix}$$

The azimuth θ is measurement clockwise from north to the principal axis $\hat{e}_2$. The detailed formulation can be found in Feigle et al. (1990, 1993) and the computation procedure is straightforward. Since we have only two years of data, we have combined several triangulations into 26 polygons to enhance the signal/noise ratio. As more sites are included in a polygon, the more reliable the strain-rate estimate is since more data will yield better estimates. The values of strain rates for each polygon are given in Table 3 and shown in terms of their average principal axes in Figure 7.

The magnitude (0.03-3.32 μstrain/yr) and pattern of principal strain rates are, in general, comparable to the observations made by Yu and Chen (1998) but with local variations. Similar to the velocity fields, strain rates increase abruptly from west to east across the CKF. In the Coastal Plain Nets A-G show both slight extension rates of 0.2-0.56 μstrain/yr and slight to moderate shortening rates 0.1-1.68 mstrain/yr. The shortening vates are on average in the E-W to ESE-WNW directions. Across the Chukou-Lunhou fault and within the Foothills belt, higher shortening rates of 0.43-3.32 mstrain/yr appear in the Nets I-S except Net O, and shortening directions follow those in the Coastal Plain. Two local distinct variations include: a) deviation of the shortening away from average regional contraction direction such as Net S, and 2) extension rates significantly greater than shortening rates such as Nets J and Q. Both features also appear commonly in the nets (Nets T to Z) across the Laonungchi fault. The local large gradients of velocity orientation and magnitude result in a change of contraction direction and the amount of extension rates. Left-lateral strike-slip motion on the Laonungchi fault may

Table 3. Horizontal principal strain rate tensors of 26 subnets in southwestern Taiwan.

NET	$\dot{\varepsilon}_1$ (μstrain/yr)	$\dot{\varepsilon}_2$ (μstrain/yr)	θ (deg)	NET	$\dot{\varepsilon}_1$ (μstrain/yr)	$\dot{\varepsilon}_2$ (μstrain/yr)	θ (deg)
CKF West				N	0.14	-1.01	107.5
A	-0.45	-0.75	87.0	CKF East			
B	0.29	-0.10	55.8	O	0.57	-0.07	-36.1
C	0.52	-1.17	107.6	P	0.56	-0.43	128.6
D	-0.33	-0.55	81.8	Q	1.66	-0.47	98.7
E	0.36	-0.55	74.8	R	0.37	-3.32	99.9
F	0.56	-0.27	110.8	S	1.28	-1.57	71.9
G	0.20	-0.27	52.5	Across Laonungchi Fault			
Across CKF				T	0.20	-0.62	115.6
H	0.28	-1.68	114.4	U	1.16	-0.35	105.7
I	-0.03	-0.71	28.7	V	0.46	-1.11	29.0
J	1.33	-0.43	-25.7	W	1.80	-0.64	128.2
K	0.28	-1.23	104.2	X	-0.43	-0.97	10.9
L	0.19	-1.40	97.9	Y	0.10	-0.29	103.9
M	0.89	-1.54	103.2	Z	1.66	-0.32	-13.2

$\dot{\varepsilon}_1$, $\dot{\varepsilon}_2$: positive for extension and negative for contraction

θ: ε_2 azimuth, positive for clockwise and negative for counterclockwise

have contributed to such changes in the nets along the fault trace. This hypothesis can be tested as more data are collected. Furthermore, Yu and Chen (1998) have shown a systematic increase in the shortening strain rates from north to south in the nets across the foothills region. Although the same trend appears locally in the nets across the Chukou-Lunhou fault, we have not found such a consistent trend along the entire trace of frontal structures in our preliminary results.

5. DISCUSSIONS AND CONCLUSIONS

Section B-B' (Figure 2) shows that the vertical components of the thrust displacements are significant compared to the horizontal components. In our interpretation, the crustal thickening is achieved by stacking of imbricated thrust faults which are rooted in a basal décollement.

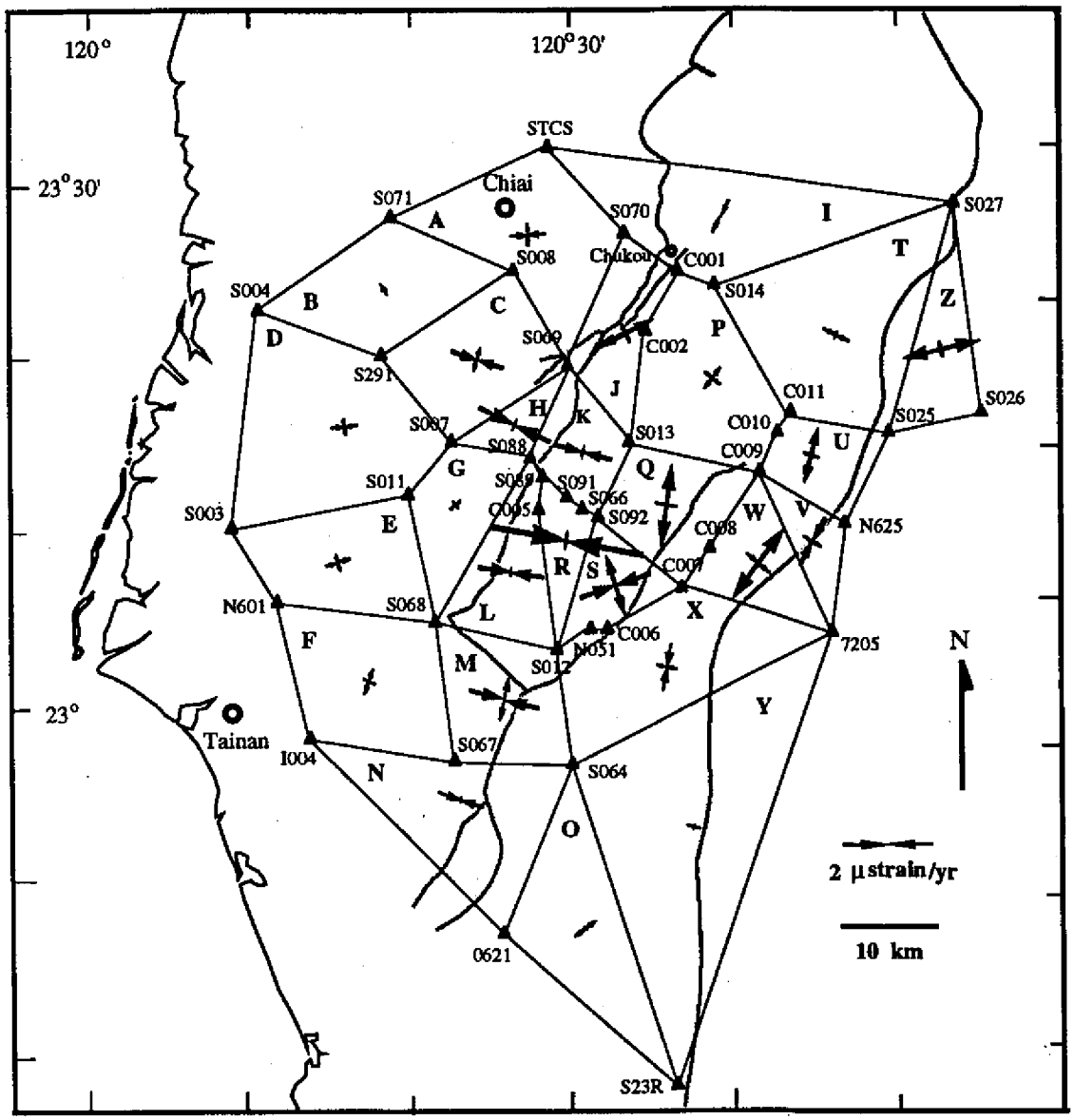

Fig. 7. Principal axes of the horizontal strain rate tensors for 26 subnets in southwestern Taiwan. In each polygon, the inward pointing arrows represent compression; outward pointing arrows represent extension. Values for all strain rates are given in Table 3.

Alternatively, other permissible structural models may include thick-skinned tectonics (e.g., Wu et al., 1997) in which high-angle reverse faults are inverted from normal faults developed during rifting stages. In addition, since both the earthquake cycle and mechanical behavior on faults are not well understood in the study area, the geodetic strain rates may reflect either an interseismic strain accumulation or strain release by aseismic creep on faults. Since the seismicity in the study area is not significant (Yu and Chen, 1998), the high strain rates observed in section E-E' may be due to aseismic slip on décollements of the Lunhou and the underlying blind fault (Figure 2).

From previous analyses of the GPS determined surface kinematics in the Fold and Thrust Belt of southwestern Taiwan, except for the local variations mentioned above, there appears to be a comparable correlation between the horizontal velocity field from our data (Figure 6) and the strain field from previous studies (in Yu and Chen, 1998, figure 5). That is, the magnitudes of both velocity and strain rates increase progressively from north to south along the vicinity of the surface trace of the Chukou-Lunhou fault. A natural question is what causes this systematic change of surface kinematics of thrust sheets. A broad view of this pattern would be that the oblique arc-continent collision is developed progressively from north to south; nevertheless, our dense cross sections suggests that the development of structures over a short distance may have a profound effect on the thrusting kinematics. For example, the surface motion of thrust sheets may be explained by, 1) the buttressing of pre-existing normal faults and "basement" highs and, 2) thick, relatively strong pre-Miocene sections involved in the deformation in the north in contrast to thick, weaker Plio-Pleistocene sections within the basin to the south (Wiltschko et al., 1997).

Contrary to previous beliefs that the CKF is a major active fault responsible for the earthquakes in southwestern Taiwan, the eastward increase of horizontal velocity along the profile E-E' implies that faults to the east of CKF may also be active or that there exists a common décollement shared by all faults at depth or both. This demonstrates that repeated surface GPS data can, in turn, constrain a structural model to interpret the subsurface structure (for example, Yeats, 1993). Furthermore, recognition that the strain is distributed over an area wider than just the CKF is important since the earthquake hazard assessment methodology must differ considerably depending on whether the deformation is localized on a few major faults or distributed widely on many structures.

Acknowledgments We thank Dr. Yu Shui-Beih of the Institute of Earth Sciences at Academia Sinica for providing the GPS data from the on-line static stations and for early help in initiating our project. Dr. Liu Chi-Ching of Academia Sinica collaborated on our project by helping with the equipment during GPS field surveys and by sharing data. The interpretation of regional geology and seismic profiles benefits from fruitful discussion with Dr. Lu ming-tar and Mr. Hsu Chin-Yun of the Chinese Petroleum Corporation, Exploration Department. Reviewed by Dr. Lin Chi-weii and one anonymous reviewer helps to clarify earlier versions of this manuscript. This study was supported by three year grants to JH from National Science Council, R.O.C. (NSC84-2111-M-008-038, NSC85-2111-M-008-037Y and NSC86-2116-M-008-008Y)

and the National Science Foundation, U.S.A. grant EAR-9506433 to DVW.

REFERENCES

Bevis, M., F. W. Taylor, B. E. Schutz, and S. Calmant, 1993: Geodetic observations of convergence and back-arc spreading in the S.W. Pacific (1988-1992). EOS. *Am. Geophys. Union Trans.*,**74**, 60.

Bonilla, M. G., 1975: A review of recently active faults in Taiwan. U.S. Geol. Survey-Open File Report, 75-41, 58pp.

Boucher, C., Z. Altamini, M. Feissel, P. Sillard, 1996: Results and Analysis of the ITRF94. IERS Technical Note 20, Observatorie de Pairs.

Chang, S. L., 1963: Regional stratigraphic study of Pleistocene and upper Pliocene formations in Chiayi and Hsinying area, Taiwan. *Petrol. Geol. Taiwan*, **2**, 65-86.

Chang, S. L., 1964: Regional stratigraphic study of Lower Pliocene and upper Miocene formations in Chiayi and Hsinying area, Taiwan. *Petrol. Geol. Taiwan*, **3**, 1-20.

Chang, Y. L., C. I. Lee, C. W. Lin, E. W. Mao, and C. H. Hsu, 1996: Inversion tectonics in the fold-thrust belt of the foothills of the Chiayi-Tainan area, southwestern Taiwan. *Petrol. Geol. Taiwan*, **30**, 163-176.

Chang, L. S. and Y. T. Yeh, 1981: A source model of the Paiho, Taiwan earthquake from the inversion of teleseismic body waveforms, National Science Council Rep., Taiwan, 65pp.

Cheng, S. N., and Y. T. Yeh, 1989: Earthquake Catalog in Taiwan Region from 1604 to 1988. Inst. Earth Sci., Academia Sinica, 255pp.

Chi, W. R., 1980: Calcareous nannoplankton biostratigraphy study and correlation of the Late Neogene sequence in the Chiayi and Hsinying foothills, southern Taiwan. *Proc. Geol. Soc. China*, **23**, 16-28.

Chinese Petroleum Corporation, 1986: Geologic map of western Taiwan, Chia-I sheet (1: 100,000). TPED, CPC, Miaoli, Taiwan.

Chinese Petroleum Corporation, 1989: Geologic map of western Taiwan, Tai-Nan sheet (1: 100,000). TPED, CPC, Miaoli, Taiwan.

Chow, J. D., J. W. Yuan, and K. M. Yang, 1986: Geological interpretation of the seismic data in the Houpi area, Tainan. *Petrol. Geol. Taiwan*, **22**, 27-53.

Chow J. D., K. M. Yang, and H. M. Chen, 1987: Structural traps of the Paiho area, southern Taiwan. *Petrol. Geol. Taiwan*, **23**, 13-40.

Couzens, B. A., and D. V. Wiltschko, 1996: The control of mechanical stratigraphy on the formation of triangle zones. *Bull. Can. Petrol. Geol.*, **44**, 165-179.

Feigle, K. L., R. King, and T. H. Hordan, 1990: Geodetic measurement of tectonic deformation in the Santa Maria fold and thrust belt, California. *J. Geophys. Res.*, **95**, 2679-2699.

Feigle, K. L., D. Agnew, Y. Bock, D. Dong, A. Konnelan, B. Hager, T. Herring , D. Jackson, T. Jordan, R. King, K. Larsen, M. Murray, Z. Shen, and F. Webb, 1993: Space geodetic measurement of crustal deformation in central and southern California. *J. Geophys.*

Res., **98**, 21677-21712.

Herring, T. A., 1998: GLOBK: Global Kalman filter VLBI and GPS analysis program Version 4.17, Internal Memorandum, Massachusetts Institute of Technology, Cambridge.

Ho, C. S., 1988: An Introduction of the Geology of Taiwan, Explanatory Text of the Geologic Map of Taiwan. Central Geol. Survey, MOEA, Taipei, 192pp.

Hsu, C. H, W. R. Chi, Y. K. Tsan, and C. C. Liu, 1980: Hydrocarbon migration and stratigraphic correlation of the Neogene formations in the Foothills of southwestern Taiwan. CPC internal report, 21pp. (in Chinese)

Hsu, C. Y., and S. K. Wei, 1983: Structural geology in the Chiayi foothills, Taiwan. *Petrol. Geol. Taiwan*, **19**, 17-28.

Hu, C. C., 1985: A study on the geologic structures of the pre-Miocene under west-central Taiwan through inversion of gravity and magnetic data. Ph.D., Disser., National Central university, Taiwan, 129pp.

Huang, C. S., H. C. Chang, and H. C. Liu, 1994: Geological investigation of the Chukou fault, southern Taiwan. *Bull. Central Geol. Survey, MOEA*, **9**, 51-76. (in Chinese)

Hung, J. H., 1995: Deformation of a thrust sheet over frontal-transverse ramps: a clay model study. *J. Geol. Soc. China*, **38**, 315-334.

Hung, J. H., 1996: Reactivation of normal faults in the fold-thrust belt of Taiwan. *EOS*, **77**, F719.

King, R. W., and Y. Bock, 1995: Documentation of the GAMIT GPS Analysis Software version 9.3, Mass. Inst. of Technol., Cambridge.

Lin, C. H., Y. H. Yeh, B. S. Huang, R. C. Shih, H. L. Lai, C. S. Huang, S. S. Yu, H. Y. Yen, C. S. Liu, and F. T. Wu, 1997: Deep crustal structures inferred from wide-angle seismic reflection data. Inter. Conf. and Sino-Am. Symp. on Tectonics of East Asia, prog./abs., 155.

Lin, H. C., 1996: Structural geology in the Foothills belt of Chianan area, southwestern Taiwan. Msc. thesis, 104pp. (in Chinese).

Mao, E. W., T. Hsu, and M. Wu, 1994: Hydrocarbon potential in the Paleogene half-graben basin of the Peikang Platform. CPC internal report, 49pp. (in Chinese)

Mitra, S., 1993: Geometry and kinematic evolution of inversion structures. *Am. Asso. Petrol. Geol.*, **77**, 1159-1191.

Morley, C. K., 1986: A classification of thrust fronts. *Am. Asso. Petrol. Geol.*, **70**, 12-25.

Mouthereau, F., J. Angelier, B. Deffontaines, Lacombe, O., H. T. Chu, B. Colletta, J. Déramond, M. S. Yu, and J. F. Lee, 1996: Present and recent kinematics of the Taiwan collision front. *C.R. Acad. Sci., Paris, t.* **323**, 713-719.

Niell, A. E., 1996: Global mapping functions for the atmospheric delay. *J. Geophys. Res.*, **101**, 3227-3246.

Reilinger, R. E., S. C. McClusky, M. B. Oral, R. W. King, M. N. Toksoz, A. Barka, I. Kinik, O. Lenk, and I. Sanli,1997: Global positioning system measurements of present-day crustal movements in the Arabia-Africa-Eurasia plate collision zone. *J. Geophys. Res.*, **102**, 9983-10000.

Serra, S., 1977: Styles of deformation in the ramp regions of overthrust faults. Wyo. Geol. Asso. Guideb., 487-498.

Shih, R. C., C. H. Lin, Y. H. Yeh, B. S. Huang, H. Y. Yen, and C. S. Liu, 1997: Stacked Images of the deep crustal structure beneath Taiwan from wide-angle seismic reflection data. Inter. Conf. and Sino-Am. Symp. on Tectonics of East Asia, prog./abs., 154.

Shin, T. C., 1995: Application of waveform modeling to determine focal mechanisms of the 1993 Tapu earthquake and its aftershocks. *TAO*, **6**, 167-179.

Sibson, R. H., 1985: A note on fault reactivation. *J. Struct. Geol.*, **7**, 751-754.

Sibson, R. H., 1995: Selective fault reactivation during basin inversion: potential for fluid redistribution through fault-valve action. In: Buchanan, J. G. and Buchanan, P. G. (Eds.), Basin Inversion. Geological Society Special Publication, 88, 3-19.

Smith, R. B., C. M. Meertens, A. M. Rubin, and N. M. Ribe, 1994: Active tectonic processes of the Yellowstone Hotspot imaged by topography, earthquakes and GPS. Geol. Soc. Am. abs./prog., 26, 313.

Sun, S. C., 1982: The Tertiary basin of offshore Taiwan. In Salivar-Sali (Ed.), Proc. Second ASCOPE Conf. Oct. 7-11, Manila, 125-135.

Suppe, J., 1976: Décollement folding in southwestern Taiwan. *Petrol. Geol. Taiwan*, **13**, 25-35.

Suppe, J., 1980: Imbricated structure of western foothills belt, southcentral Taiwan. *Petrol. Geol. Taiwan*, **17**, 1-16.

Wiltschko, D. V., and D. B. Eastman, 1983: A photoelastic study of the effects of preexisting reverse faults in basement on the subsequent deformation of the cover. *Geol. Soc. Am., Memoir,* **171**, 111-117.

Wiltschko, D. V., J. H. Hung, J. B. Hickman, C. Liu, S. B. Yu, and P. Fang, 1997: Structure and motion of the frontal portion of the southern Taiwan Fold and Thrust Belt. Inter. Conf. and Sino-Am. Symp. on Tectonics of East Asia, prog./abs., 134.

Wu, F. T., Y. H. Yeh, and Y. B. Tsai, 1979: Seismicity in the Tsenwen reservoir area, Taiwan. *Bull. Seis. Soc. Am.*, **69**, 1783-1796.

Wu, F. T., R. J. Rau, and D. Salzberg, 1997: Taiwan Orogeny, thin-skinned or lithospheric collision, *Tectonophysics*, **274**, 191-220.

Yeats, R. S., 1993: Converging more slowly. *Nature*, **366**, 299-231.

Yeh, M, W. S. Chen, and W. C. Shih, 1997: Recognition and interpretation of sequence stratigraphy by seismic, Pliocene-Pleistocene, southwest plain, Taiwan. Symp. on Stratigraphy and Geology in Southwestern Taiwan, abs./ prog., 53-57. (in Chinese)

Yeh, Y. H., and H. Y. Yen, 1992: Bouger anomaly map of Taiwan. Inst.. Earth Sci., Academia Sinica, Taipei, Taiwan, R.O.C.

Yu, S. B, 1993: Monitoring of active faults in southwestern Taiwan (III). National Science Council Rep., 81-0414-p001-02B, 39 pp. (in Chinese)

Yu, S. B., and H. Y. Chen, 1994: Global positioning system measurements of crustal deformation in the Taiwan arc-continent collision zone. *TAO*, **5**, 477-498.

Yu, S. B., and H. Y. Chen, 1998: Strain accumulation in southwestern Taiwan. *TAO*, **9**, 31-50.

Yuan, C. W., I. C, Lin, S. T. Huang, and C. L. Hsiao, 1984: Petrology and sedimentary environment of pre-Miocene strata in the Peikang area, Taiwan. CPC internal report, 83pp. (in Chinese)

Yuan, C. W., S. T. Huang, D. F. Chou, R. C. Wu, and T. L. Lu, 1987: A geologic study of high pore-pressure zones in southern Taiwan. CPC, Exploration and Development Research Center, 89pp. (in Chinese)